# Quantum supercavity with atomic mirrors

Lan Zhou (周兰),[1,2] H. Dong (董辉),[3] Yu-xi Liu (刘玉玺),[1,4] C. P. Sun (孙昌璞),[1,3] and Franco Nori (野理)[1,4,5]
[1]*Advanced Science Institute, The Institute of Physical and Chemical Research (RIKEN), Wako-shi 351-0198, Japan*
[2]*Department of Physics, Hunan Normal University, Changsha 410081, China*
[3]*Institute of Theoretical Physics, The Chinese Academy of Sciences, Beijing, 100080, China*
[4]*CREST, Japan Science and Technology Agency, Kawaguchi, Saitama 332-0012, Japan*
[5]*Center for Theoretical Physics, Physics Department, Center for the Study of Complex Systems, University of Michigan, Ann Arbor, Michigan 48109-1040, USA*

(Received 25 September 2008; published 16 December 2008)

We study single-photon transport in an array of coupled microcavities where two two-level atomic systems are embedded in two separate cavities of the array. We find that a single photon can be totally reflected by a single two-level system. However, two separate two-level systems can also create, between them, single-photon quasibound states. Therefore, a single two-level system in the cavity array can act as a mirror while a different type of cavity can be formed by using two two-level systems, acting as tunable "mirrors," inside two separate cavities in the array. In analogy with superlattices in solid state physics, we call this "cavity inside a coupled-cavity array" a supercavity. This supercavity is the quantum analog of Fabry-Perot interferometers. Moreover, we show that the physical properties of this quantum supercavity can be adjusted by changing the frequencies of these two-level systems.

DOI: 10.1103/PhysRevA.78.063827 PACS number(s): 42.50.Pq, 32.80.Qk, 73.22.Dj, 85.85.+j

## I. INTRODUCTION

In quantum networks, photons provide faithful quantum-information transfer, because they travel at the speed of light over long distances, and with little decoherence compared to other information carriers (e.g., electrons). To interconnect networks, it is crucial to have a quantum memory at the switching nodes. Many approaches have been proposed to realize quantum memories, where quantum information can be stored and retrieved, for instance, using electromagnetically induced transparency (e.g., in Refs. [1–3]) or photon echoes (e.g., Refs. [4–6]). Photons can be confined to a very small volume (e.g., Ref. [7]) using microcavities or microresonators with low dissipation and thus the microcavities can serve as quantum memories. Moreover, experiments also demonstrated that the quality factor of a photonic crystal nanocavity [8,9] or microwave cavity [10,11] can be controlled by dynamically changing the environment of the cavity.

To faithfully transfer quantum information, individual photon control would be desirable. Single-photon turnstiles have been studied in, e.g., Refs. [12–14]. There, a semiconductor quantum dot [12] or a single atom [13,14] can behave as a photon turnstile. Recently, a nonlinear two-photon switch device using nanoscale surface plasmons has been [15] theoretically studied, where a single-photon gate is used to control the propagation of subsequent single photons. Considering the one-dimensional scattering process of single-photons by a two-level system, the total reflection can be controlled by tuning the inner structure of the scatterer [16–18]. A solid state device, functioning as a single-photon quantum switch [19,20] in a one-dimensional coupled-cavity waveguide has been studied, also using a discrete-coordinate approach [17].

For single-photon transport in a one-dimensional waveguide, the photons can be totally reflected [16–18] by a controllable two-level system which can act as a perfect mirror. It is known that the Fabry-Perot cavity, which consists of two highly reflecting planar mirrors, is the simplest cavity. It is then natural to ask the question: "is it possible to construct a *quantum resonator*, in a one-dimensional waveguide, with two controllable quantum scatterers?" Here, we focus on this question and study *quantum analogs of the Fabry-Perot cavity* .

This paper studies the coherent transport of photons, which propagate in a one-dimensional coupled-resonator waveguide (CRW) and are scattered by two controllable two-level systems located separately in the CRW. Besides presenting a unified theory, including both the long-wavelength and short-wavelength regimes, the discrete coordinate approach employed in this work shows the following:

(1) Photon quasibound states, with a tunable leakage, appear in the region sandwiched between the two two-level systems, when the interaction between the two-level systems and the cavity field is strong compared with the hopping constant. (Hereafter, for brevity, we will often use the word "atom" instead of "two-level system." In the terminology of quantum information, a two-level system is a qubit, therefore, hereafter, a two-level system is sometimes called a qubit, but this "atom" refers to an artificial atom made, e.g., from a superconducting circuit.)

(2) A perfect quantum supercavity, confining photons inside the two "atoms," can be formed when the transition energies of these two-level systems are equal to the photon energy, with wave number $k=n\pi/(2d)$, where $2d$ is the distance between the two atomic scatterers and $n$ is an integer.

(3) Photons can be stored and reemitted by adjusting the transition frequencies of these two two-level systems.

This paper is organized as follows: In Sec. II, we present our model, a coupled-cavity array with two atoms separately embedded in two different cavities. In Sec. III, we study the transport properties of a single-photon, and derive the condi-

 

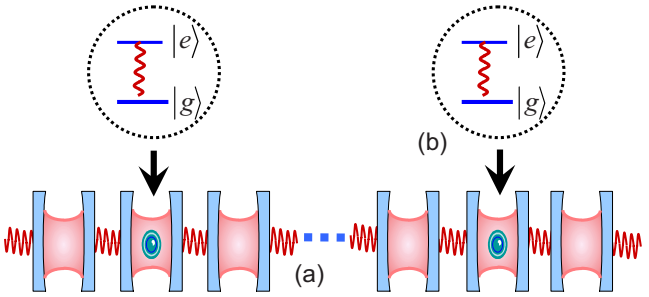


FIG. 1. (Color online) Schematic configuration for a quantum supercavity realized by two atoms embedded in two separated cavities of a coupled resonator waveguide, as shown in (a). Each atom can be represented as in (b). These two atoms can behave as two partly reflecting mirrors, forming a cavity-within-a-cavity, or supercavity. This can act as a quantum analog of Fabry-Perot interferometer.

tions for the coherent control of a single-photon scattering by two atoms. In Sec. IV, the quantum supercavity, with *two atomic mirrors*, is studied. We prove that the leakage of this supercavity is tunable by changing the transition energy of these two atoms. The wave numbers inside this supercavity are also analytically obtained by a perturbation approach. Moreover, we study how a supercavity can be formed in the long-wavelength (low-energy) regime in Sec. V and in the short-wavelength (higher-energy) regime in Sec. VI. These two regimes correspond to the quadratic and linear photon dispersion relation, respectively. Conclusions are summarized at the end of the paper.

## II. MODEL

As shown in Fig. 1, we consider a one-dimensional coupled-resonator waveguide (CRW) with two two-level systems, embedded separately in two distant cavities. The CRW can be either an array of coupled superconducting transmission line resonators or an array of coupled defect resonators in photonic crystals (see, e.g., Ref. [21]). The two-level systems can be either natural atoms or artificial atoms (e.g., superconducting qubits or semiconducting quantum dots).

In contrast to the similar configurations in Refs. [22–26], here only two atoms are located inside the CRW.

Once a photon is inside one cavity of the CRW, it propagates along the CRW and is also scattered by the atoms. The CRW can be described by the Hamiltonian

$$H_c = \omega \sum_{j=-\infty}^{\infty} a_j^\dagger a_j - \xi \sum_{j=-\infty}^{\infty} (a_j^\dagger a_{j+1} + \text{H.c.}) \tag{1}$$

with the annihilation operator $a_j$ and creation operator $a_j^\dagger$ of the $j$th cavity mode. The first term of Eq. (1) denotes the free Hamiltonian of all the resonators. The second term of Eq. (1) represents the couplings between any two nearest-neighbor cavities. For example, $a_j a_{j+1}^\dagger$ means that the photon is annihilated in the $j$th cavity and is created in the $(j+1)$th cavity. Here, for simplicity, we assume that all resonators have the same frequency $\omega$ and the hopping energies $\xi$ between any two nearest-neighbor cavities are the same. The hopping energy $\xi$ is determined by the intercavity coupling. $H_c$ is a typical tight-binding boson model and can be rewritten as

$$H_c = \sum_k E_k b_k^\dagger b_k \tag{2}$$

by introducing the Fourier transform

$$b_k = \frac{1}{\sqrt{N}} \sum_j e^{ikj} a_j. \tag{3}$$

The dispersion relation between $E_k$ and $k$ is given by

$$E_k = \omega - 2\xi \cos k, \tag{4}$$

which forms an energy band. Here, the lattice constant $l$ is set to unity.

Let us assume that each atom has a ground state $|g\rangle$ and an excited state $|e\rangle$. Let the distance between the two atoms embedded in the CRW be $2d$. For convenience, we take the 0th cavity as the coordinate-axis origin. As shown in Fig. 1, we also assume that the first atom, with transition energy $\Omega_1$, is located at the $(-d)$th cavity, on the left-hand side of the origin, and the second atom, with transition energy $\Omega_2$, is embedded in the $d$th cavity, on the right-hand side of the origin. Under the rotating-wave approximation, the interaction between the $d$th and $(-d)$th cavity fields and the two atoms is described by the Jaynes-Cummings Hamiltonian

$$H_I = \sum_{l=1,2} [\Omega_l |e\rangle_l\langle e| + J_l (|e\rangle_l\langle g| a_{(-1)^l d} + \text{H.c.})], \tag{5}$$

where $J_l$ is the coupling strength between the $l$th atom and the $(-1)^l d$th cavity field.

The total Hamiltonian $H = H_I + H_c$ exihibits different behaviors in the long-wavelength (low-energy) regime and the short-wavelength (higher-energy) regime, which correspond to the quadratic and linear regimes of the photon dispersion relation, respectively. Namely, in the low-energy regime, the long-wavelength approximation gives a photon quadratic spectrum

$$E_k \simeq \omega - 2\xi + \xi k^2, \tag{6}$$

while in the higher-energy regime, the short-wavelength approximation leads to a photon linear spectrum

$$E_k \simeq \omega - \pi\xi \pm 2\xi k. \tag{7}$$

Both regimes will be studied in this paper.

We note that an ideal system without losses is considered here. In practice, both photons and atoms unavoidably interact with different environments, that is, dissipation always exists. The dissipation substantially reduces the propagating length of the photons, and so does the transmission of the single photon. In order to present the main physics of this system, we neglect dissipation, decoherence, and the nonuniform couplings in this paper. These effects are separately studied and will be presented in the future.

## III. SINGLE-PHOTON REFLECTION AND TRANSMISSION

A photon incident from the left of the CRW, with energy within the energy band, propagates along the one-

dimensional CRW until it is scattered by the first atom. Then it splits into transmitted and reflected portions. The transmitted part propagates freely until it encounters the second atom, where the same type of splitting occurs once again.

In this section, we will discuss the reflection and transmission coefficients of a single photon in terms of the projection of the asymptotic wave packets onto appropriate plane waves. First, we consider the eigenstates of the total system. Three mutually exclusive possibilities are considered: Either the photon is propagating inside the cavity, or the photon is absorbed by one atom or the other. Considering all three cases, the stationary state for the Hamiltonian $H=H_I+H_c$ is written in the form

$$|E_k\rangle = \sum_j u_k(j)a_j^\dagger|0gg\rangle + u_{1e}^k|0eg\rangle + u_{2e}^k|0ge\rangle, \tag{8}$$

where the first number 0 inside the Dirac brackets represents the vacuum state of all cavity fields. The parameter $u_k(j)$ represents the probability amplitude for finding the photon at the $j$th cavity. $u_{le}^k$ is the probability amplitude of the $l$th atom in its excited state while the other atom is in the ground state and all the cavity fields are in the vacuum. This form of $|E_k\rangle$ includes the three cases listed above. Using the Schrödinger equation, the single-photon scattering process can be described by the following equation:

$$\begin{aligned}(E_k-\omega)u_k(j)+\xi[u_k(j+1)+u_k(j-1)]\\ = J_1G_{1k}\delta_{j(-d)}u_k(-d)+J_2G_{2k}\delta_{jd}u_k(d),\end{aligned} \tag{9}$$

where the Green function $G_{lk}=J_l/(E_k-\Omega_l)$ is obtained from the relation

$$u_{le}^k = \frac{J_l}{E_k-\Omega_l}u_k[(-1)^l d]. \tag{10}$$

If we regard the second term of the left-hand side of Eq. (9) as the kinetic energy term and the right-hand side of Eq. (9) as potential energy term, then Eq. (9) describes the eigenfunction $u_k(j)$ subjected to a potential with singularities at $j=\pm d$. In the region $j\neq\pm d$, the potential is zero, the solutions to Eq. (9) are plane waves with wave vectors $k$. Therefore, we consider the wave functions

$$u_k(j) = \begin{cases} e^{ikj}+re^{-ikj}, & j<-d,\\ Ae^{ikj}+Be^{-ikj}, & -d<j<d,\\ te^{ikj}, & j>d.\end{cases} \tag{11}$$

The $u_k(j)$ in Eq. (11) describes the scattering process of an initial plane wave $\exp(ikj)$ incident from the left-hand side of $j=-d$. This freely propagating wave is either reflected or transmitted when it encounters the first scatterer. The reflection and transmission are described by the amplitudes $r$ and $A$. The transmitted wave propagates freely until it encounters the second scatterer at the point $j=d$, where the corresponding reflection and transmission amplitudes are described by $B$ and $t$. Here both scatterers produce a highly localized repulsive or attractive effective force, which depends on the incident energy of the single photon, the transition energies of the atoms, and the coupling strength between the atoms and their corresponding cavities.

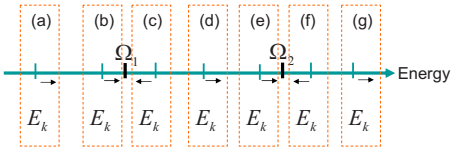


FIG. 2. (Color online) This figure schematically illustrates seven different cases (a)–(g) discussed in the text and also corresponding to the seven cases (a)–(g) in Fig. 3. Here $E_k$ is the photon energy, and $\Omega_1$,$\Omega_2$ are the two atomic transition energies. The arrows indicate when the photon energy $E_k$ increases or decreases. In (a) $E_k<\Omega_1$; (b) $E_k$ is slightly below $\Omega_1$, and increasing; (c) $E_k$ is slightly above $\Omega_1$, and decreasing; (d) $\Omega_1<E_k<\Omega_2$; (e) $E_k\to\Omega_2$; (f) $E_k$ approaches $\Omega_2$ from the right-hand side, (g) $E_k$ moving away from $\Omega_2$.

### A. Atomic transition energy $\Omega_l$ inside the band

Figure 2 schematically illustrates the seven cases (a)–(g) shown in Fig. 3. Figure 3 shows how the potential energy depends on the energy $E_k$ of the incident photon. All the results schematically shown in Fig. 3 are derived directly from Eq. (9). Here, we assume $\Omega_1<\Omega_2$ and both transition energies $\Omega_l$ ($l=1,2$) are in the region $[\omega-2\xi,\omega+2\xi]$. When the photon energy $E_k<\Omega_1$ is smaller than the transition energy of the first atom, two attractive $\delta$ function potentials

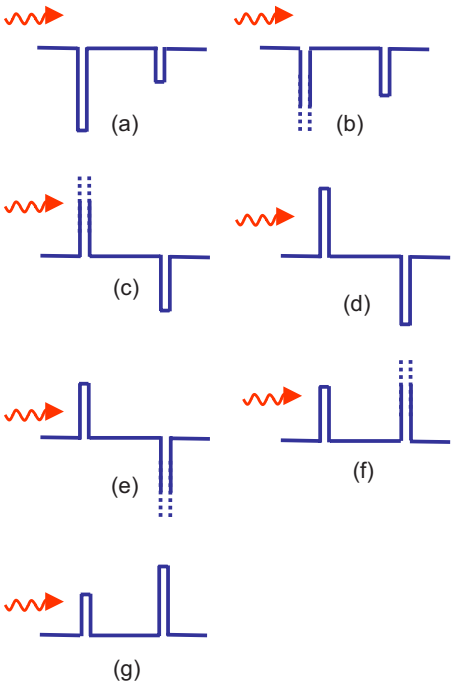


FIG. 3. (Color online) Schematic diagrams of the single-photon scattering process with $\Omega_1<\Omega_2$ inside the energy band. Here, the vertical axis is energy and the horizontal axis is the position along the CRW. Also, $\Omega_l$ is the transition energy of the $l$th atom ($i=1,2$). The dashed lines refer to an infinitely high potential barrier or well. The seven cases (a)–(g) shown here correspond to the seven photon energy regimes (a)–(g) explained in Fig. 2. The cases (b), (c), (e), and (f) correspond to the total reflection of the incident photon because in each one of these cases one of the wells or barriers is infinite.

appear at $j=\pm d$ [as schematically shown in Figs. 2(a) and 3(a)]. If the photon energy $E_k$ is increased and approaches $\Omega_1$, Figs. 2(b) and 3(b), the potential located at $j=-d$ tends to minus infinity. However, when $E_k$ approaches $\Omega_1$ from the right-hand side, as shown in Figs. 2(c) and 3(c), the first potential gradually becomes an infinite barrier. When the incident photon energy $E_k$ is further increased and is between $\Omega_1$ and $\Omega_2$, Fig. 2(d), photons first collide with a repulsive finite potential, then go through an attractive potential well, as schematically shown in Fig. 3(d). As $E_k$ further increases, Fig. 2(e), the height of the potential barrier at $j=-d$ becomes lower and lower, and the second two-level system creates a potential well with its depth becoming deeper and deeper, Fig. 3(e), eventually becoming a potential well with infinite depth. After $E_k$ goes across the transition energy $\Omega_2$, Fig. 2(f), a double-barrier is produced by the atoms, as shown in Fig. 2(f). In this case, the waves are totally reflected when the height of the $\delta$ potential of the second atom, goes to infinite, Fig. 3(f). Figure 3(g) shows the potential energy corresponding to the energies shown in Fig. 2(g). Therefore, Fig. 3 schematically presents ways to control photon transport by, e.g., adjusting the transition frequencies, $\Omega_1$ and $\Omega_2$, of the two atoms.

From the continuity conditions $u_k(\pm d^+)=u_k(\pm d^-)$ and the eigenvalue equations

$$(E_k-\omega-J_2G_{k2})u_k(d)=-\xi[u_k(d+1)+u_k(d-1)], \quad (12)$$

$$(E_k-\omega-J_1G_{k1})u_k(-d)=-\xi[u_k(-d+1)+u_k(-d-1)] \quad (13)$$

at $j=\pm d$, the transmission amplitude $t$ can be derived,

$$t=4\xi^2\sin^2 k\Big((e^{i4kd}-1)J_1G_{k1}J_2G_{k2}+2i\xi\sin k\sum_l J_lG_{kl}+4\xi^2\sin^2 k\Big)^{-1}. \quad (14)$$

Above, $d^{\pm}=d\pm\epsilon$, where $\epsilon$ is a very small positive number. When the photon frequency $E_k$ matches one of the atomic transition frequencies $\Omega_l$ ($l=1,2$), the transmission $t$ is zero. This $t=0$ case occurs in cases (b), (c), (e), and (f) in Figs. 2 and 3. When an atom has its transition energy $\Omega_l$ inside the energy band, it may be excited by the incident photon. The absorption or emission of a photon by an atom leads to wave interference between the incident wave and the reflected wave.

### B. Atomic transition energy $\Omega_l$ outside the band: $\Omega_l<\omega-2\xi$, $\Omega_l>\omega+2\xi$

For an atom with transition energy $\Omega_l$ far away from the energy band, the propagating single photon cannot excite the atom, thus the photon emerges in the other side of the scatterers with its energy (almost) equal to its original one, due to energy conservation.

Using Eq. (14), in Fig. 4, we plot the reflection coefficient $R=1-T$ (blue solid line) and the transmission coefficient $T=|t|^2$ (red dashed line) as a function of the incident photon wave number $k$ ($-\pi\leqslant k\leqslant\pi$), when both atomic transition

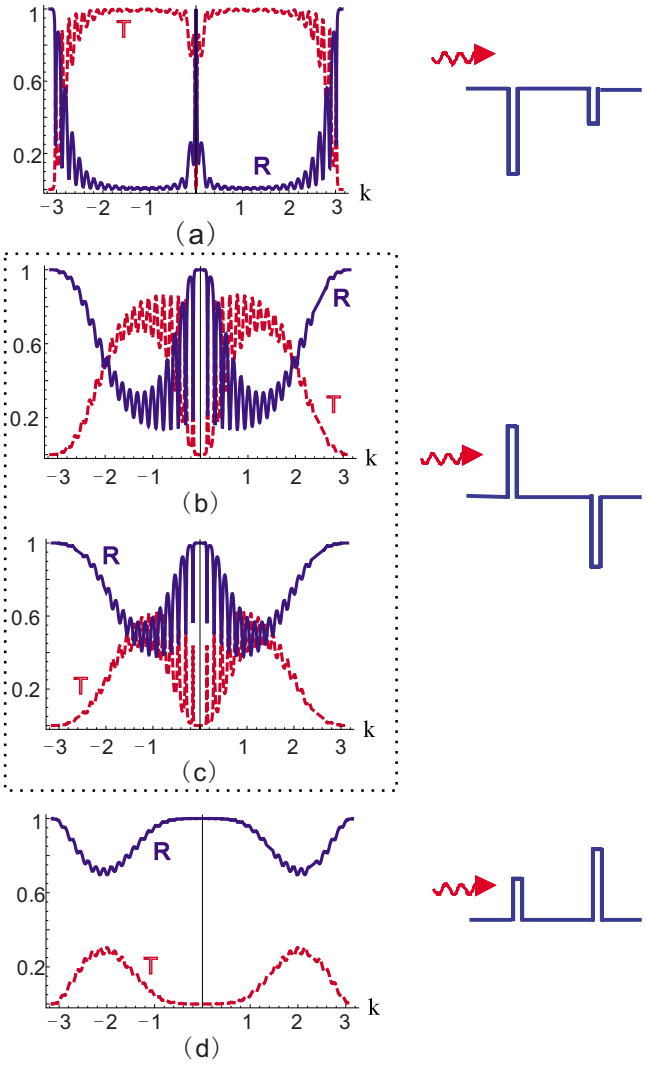


FIG. 4. (Color online) The photon reflection coefficient $R=1-T$ (blue solid line) and the photon transmission coefficient, $T$ (red dashed line) as a function of the photon wave number $k$ ($-\pi\leqslant k\leqslant\pi$) when both atomic transition frequencies $\Omega_l$ are outside the band $[\omega-2\xi,\omega+2\xi]$. Here, $k$ and $d=10$ are in units of the lattice constant, and other parameters are in units of $\xi$. Here, the cavity energy is $\omega=5$, (a) $\Omega_1=8$, $\Omega_2=8$, and the coupling between the atoms and the CRW are $J_1=0.5$, $J_2=0.7$; (b) $\Omega_1=2$, $\Omega_2=8$, $J_1=0.7$, $J_2=2$; (c) $\Omega_1=2$, $\Omega_2=8$, $J_1=0.7$, $J_2=2.6$; (d) $\Omega_1=2$, $\Omega_2=2.7$, $J_1=0.5$, $J_2=3$. Panel (a) corresponds to two potential wells at $j=\pm d$. Panels (b) and (c) correspond to one potential barrier at $j=-d$ and one potential well at $j=d$. Panel (d) corresponds to two potential barriers.

energies $\Omega_l$ are outside the energy band. As shown in Fig. 4, total reflection $R=1$ always happens at $k=0,\pm\pi$ for nonzero $J_1$ and $J_2$, and this total reflection is completely independent of the transition energies $\Omega_l$ of the atoms. This observation is caused by the following reasons. First, a band, Eq. (4), is formed in this periodic CRW, which acts like a photon filter or a photon "band-pass filter": Transmitting photons over a limited frequency range. Incident photons with energy $E_k$ outside the band do not interact with the CRW, therefore, the photon group velocities vanish at the zone boundaries or band edges. Second, when the atomic transition energies $\Omega_l$

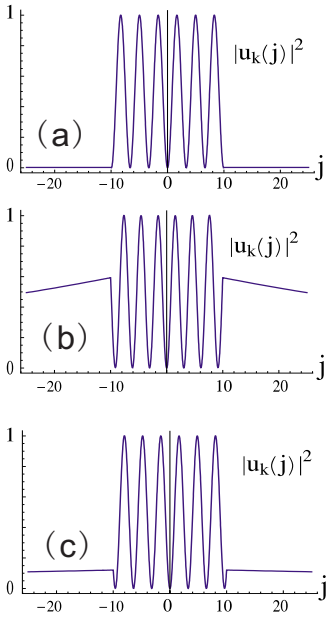


FIG. 5. (Color online) The probability $|u_k(j)|^2$ for finding the photon for a given $k$ versus the position along the CRW. The parameters are in units of $J$ and are set as follows: $d=10$, $\omega=10$, $n=3$, $\xi=0.2$, (a) $\Omega=10$, (b) $\Omega=6$, (c) $\Omega=7$. $j$ is in units of the lattice constant. For a given $n$, $q_n=n\pi/d$. These were the inputs to Eqs. (27) and (28), which provide $Q_n^L$ and $k$. With this $k$, Eqs. (19)–(22) are used to obtain the $u_k(j)$'s shown in the figures.

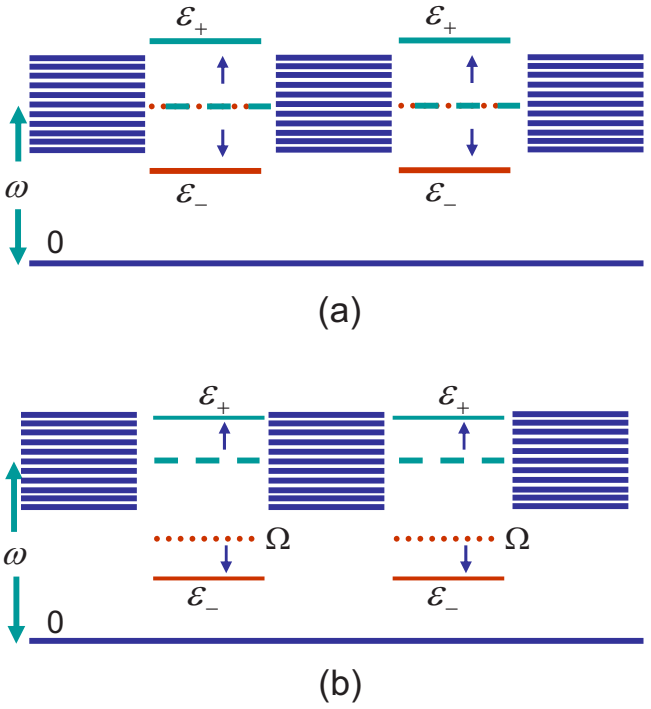


FIG. 6. (Color online) The corresponding schematic explanation for the establishment of the supercavity in Fig. 5. The eigenenergy $\omega$ of the cavities at $j=\pm d$ are shown by the green dashed lines, and the atomic transition energy $\Omega$ is shown by the red dotted line. The eigenvalues of the two dressed states are denoted by the symbols $\varepsilon_\pm$. The blue solid lines show the energy band formed by the numerous other resonators. The arrows denote the shifting of the bare eigenvalues towards their dressed values.

are outside the band, the infinite $\delta$ potential wells or barriers cannot be formed, and the total photon reflection does not occur, except when $k=0,\pm\pi$.

The oscillations shown in $T(k)$ and $R(k)$ in Fig. 4 originate from the multiple interference of waves in the region sandwiched by the two atoms. Comparing Figs. 4(a) and 4(b), we find that as the coupling strengths $J_l$ between the atoms and the CRW increase ($J_1$ from 0.5 to 0.7 and $J_2$ from 0.7 to 2), the oscillation in $R(k)$ becomes much larger when $|k|\leqslant 1$, i.e., increasing the coupling strengths $J_l$ magnifies the oscillations in $R(k)$ and $T(k)$. Indeed the wave interference giving rise to the oscillations in $R(k)$ and $T(k)$ varies with five parameters: The energy $E_k$ of the incident photon, the atomic energies $\Omega_l$, and the couplings $J_l$ between the atoms and the CRW. The case shown in Fig. 4(a) corresponds to two potential energy wells. The cases considered in Figs. 4(b) and 4(c) correspond to one barrier in $j=-d$ and one well in $j=d$. For the case considered in Fig. 4(d), there is a double barrier. As is well known, the reflection and transmission coefficients are the same for a $\delta$ potential barrier and a $\delta$ potential well, but their reflection and transmission amplitudes are different by a phase factor. It is this phase difference that produces the clearly visible oscillations, due to interference shown in Fig. 4.

Figure 4 shows the complex dependence of $R(k)$ and $T(k)$ as a function of the coupling strengths $J_l$, the hopping energy (or the intercavity coupling strength) $\xi$, and the detunings, $\delta_l=\omega-\Omega_l$, between the atoms and their corresponding cavities. If both coupling strengths $J_l$ are much smaller than the hopping energy $\xi$, the hopping plays a leading role. In this case, and as shown in Fig. 4(a), the transmission $T(k)$ is quite large. When either $J_l$ is larger than its corresponding detuning $\delta_l$, and also larger than $\xi$, the reflection dominates, as in Fig. 4(d). This result can also be found from the phase diagram (Fig. 4) in Ref. [17]. Figures 4(b) and 4(c) show the intermediate stage between nearly total transmission in Fig. 4(a) and nearly total reflection in Fig. 4(d). In order to make this point somewhat explicit, we now approximately write the transmission amplitude as

$$t \approx \sin^2 k\left((e^{i4kd}-1)\frac{J_1G_1}{2\xi}\frac{J_2G_2}{2\xi}+i\sin k\sum_l\frac{J_lG_l}{2\xi}+\sin^2 k\right)^{-1}$$
$$=\sin^2 k\left((e^{i4kd}-1)\frac{J_1^2}{2\xi\delta_1}\frac{J_2^2}{2\xi\delta_2}+i\sin k\sum_l\frac{J_l^2}{2\xi\delta_l}+\sin^2 k\right)^{-1}, \quad (15)$$

when the coupling strength $J_l$ is larger than the hopping energy and smaller than the corresponding detuning $\delta_l$. Here, $G_l=J_l/\delta_l$. Equation (15) shows that, when $J_l^2\gg 2\xi\delta_l$, the reflection spectrum is much larger than the transmission spectrum, which coincides with the change shown numerically from Fig. 4(b) to Fig. 4(c). Notice that in the large detuning condition ($\delta_l\gg J_l$), the magnitude $J_l^2/\delta_l$ is the shift of the energy levels due to the atom-cavity interaction (see Figs. 5 and 6). Therefore, the relation between $J_l^2/\delta_l$ and the half-width $2\xi$ of the band determines whether the reflection or the

transmission plays a dominant role. This phenomenon will become much clearer from the energy-level diagrams shown in the next section.

When the atoms embedded in $\pm d$ cavities are identical, e.g., $\Omega=\Omega_1=\Omega_2$, $J=J_1=J_2$, the transmission coefficient $T=|t|^2$ is derived from Eq. (14) as

$$T=\left[1+(JG_k)^2\left(\frac{JG_k\sin(2kd)}{2\xi^2\sin^2 k}+\frac{\cos(2kd)}{\xi\sin k}\right)^2\right]^{-1}, \quad (16)$$

where

$$G_k=\frac{J}{E_k-\Omega}. \quad (17)$$

We note that the maximum magnitude of the transmission coefficient $T$ in Eq. (16) can be achieved when one of the below conditions is satisfied: (1) The coupling strength $J$ is much smaller than the detuning $\delta_{ph}=E_k-\Omega$ between the energy $E_k$ of the incident photon and the transition energy $\Omega_l$ of each atom for a given nonzero $\xi$; (2) The coupling strength $J$ is much smaller than the hopping energy between adjacent cavities for a definite nonzero detuning $\delta_{ph}$; (3) the condition

$$\tan(2kd)=-\frac{2\xi\sin k}{JG_k}$$

is satisfied. This third leads to a resonant tunneling effect, which will be studied below.

## IV. SUPERCAVITY ON RESONANT STATES

The above results show that two atoms may act as a potential double barrier. Any potential double barrier can produce a wave function localized in space (see, e.g., [27,28]). Therefore, photons located in the range $[-d,d]$, between the two barriers, may bounce back and forth. Thus, this double-barrier forms a resonator [27]. Photons can leak out of the resonator owing to the finite width and height of the potential barriers. Therefore, the localized state formed by this potential energy double barrier is called a quasibound state or a resonant state [29–31]. A particle tunnels, through two energy barriers, when its energy matches (resonates with) the localized energy level.

In the system we consider here, the photon propagating in this system encounters a double-potential well and/or barrier, separated by a distance $2d$. Such a potential can exhibit resonances. In this section, we derive the conditions for the photons to be trapped inside the resonator formed by the two atoms. Therefore, a quantum supercavity can be formed by two atoms embedded in two separated cavities of the CRW.

### A. Photon wave function in the supercavity

For simplicity, we now assume that the atoms at $j=\pm d$ are identical, e.g., $J_1=J_2=J$ and $\Omega_1=\Omega_2=\Omega$. The eigenfunctions in this system satisfy the discrete scattering equation derived by Eqs. (12) and (13),

$$(E_k-\omega)u_k(j)=-\xi[u_k(j+1)+u_k(j-1)]+JG_k[\delta_{j-d}u_k(j)+\delta_{jd}u_k(j)]. \quad (18)$$

A resonant state is an eigenfunction of Eq. (18) under the boundary condition that only outgoing waves appear outside the potential. Therefore, we assume that Eq. (18) has the following solutions:

$$u_k(j)=\begin{cases} Ce^{-ikj}, & j<-d, \\ A_be^{ikj}+B_be^{-ikj}, & -d<j<d, \\ De^{ikj}, & j>d, \end{cases} \quad (19)$$

where the coefficients $A_b$, $B_b$, $C$, and $D$ are the amplitudes for finding the particle in the state $\exp(\pm ikj)$, respectively. We also define the normalized amplitudes via the ratios

$$b_b\equiv\frac{B_b}{A_b},\quad c\equiv\frac{C}{A_b},\quad d\equiv\frac{D}{A_b}.$$

By imposing the continuity equation $u_k(d^+)=u_k(d^-)$ and using the Schrödinger Eq. (18) at the point $j=d$, we find

$$b_b=\frac{JG_ke^{i2kd}}{2i\xi\sin k-JG_k}, \quad (20a)$$

$$d=\frac{i\xi\sin k}{2i\xi\sin k-JG_k}. \quad (20b)$$

Using the continuity equation $u_k(-d^+)=u_k(-d^-)$ and Eq. (18) at the point $j=-d$, we have

$$b_b=\left(\frac{2i\xi\sin k}{JG_k}-1\right)e^{-2ikd}, \quad (21a)$$

$$c=e^{-i2kd}\frac{i\xi\sin k}{JG_k}. \quad (21b)$$

Obviously, Eq. (20a) and Eq. (21a) must be equal, and the odd and even parities of the quasibound states in Eq. (19) are included in

$$e^{i2kd}=\pm\left(\frac{2i\xi}{JG_k}\sin k-1\right), \quad (22)$$

where the plus sign gives the even parity and the minus sign has an odd parity.

### B. Existence of quasibound states

Let us define a parameter $\lambda=2\xi/J^2$. Now we solve the transcendent equation (22) by a perturbation approach up to second order in parameter $\lambda$, e.g., $O(\lambda^2)$. First, let us assume that Eq. (22) possesses a real solution for $k$ only up to first order in $\lambda$ (this assumption will be proved later in this section). We set $k=k_{\rm re}$ for a real wave number. When $k$ is a real number

$$\cos(2k_{\rm re}d)=\mp 1, \quad (23a)$$

$$\sin(2k_{\rm re}d)=\pm\frac{2\xi\sin k_{\rm re}}{JG_{k_{\rm re}}}. \quad (23b)$$

Then the relation

$$\tan(2k_{\mathrm{re}}d) = -\frac{2\xi \sin k_{\mathrm{re}}}{JG_{k_{\mathrm{re}}}} \tag{24}$$

provides the condition for the existence of quasibound levels, which lead to the transmission coefficient $T=1$. For a resonant state with an odd parity, the momentum $k$ satisfies

$$k_{\mathrm{re}}d = n\pi - \varepsilon \tag{25}$$

due to the zero probability for finding the particle outside the barriers, where $\varepsilon$ is a small positive quantity and $n$ is an integer. Substituting Eq. (25) into the right-hand side of Eq. (24) and with the condition $J^2 \gg 2\xi$, the momentum of the resonant state can be approximately obtained as

$$k_{\mathrm{re}} = q_n - \frac{\lambda}{2d}(\delta - 2\xi \cos q_n)\sin q_n + O(\lambda^2), \tag{26}$$

where $\delta=\omega-\Omega$, and $q_n=n\pi/d$. For even-parity states, the momenta of the resonant states are similar to that in Eq. (26) with $n$ replaced by $(n+1/2)$. Equation (26) implies that discrete levels appear in the energy band. In a similar way, we can derive the discrete energy of the resonant states with even parity.

Although Eq. (29) gives the energy of a quasibound state, it fails to describe the behavior of the wave function outside the sandwiched region. Indeed, a complex wave number $k$ must be considered in order to obtain the lifetime of a quasibound state. To do this, let us come back to Eq. (22). Here we show that, to second order in $\lambda$, the imaginary part of $k$ (which can represent the lifetime of the resonant state via its dispersion relation), appears when the wave number in Eq. (26) is treated as a complex number. We obtain approximate analytical expression of the wave number

$$k = q_n - \frac{1}{2}Q_n + dQ_n^2 + i\frac{\lambda}{2d}Q_n[\delta \cos q_n - 2\xi \cos(2q_n)] + O(\lambda^3), \tag{27}$$

where

$$Q_n = \frac{\lambda}{d}(\delta - 2\xi \cos q_n)\sin q_n. \tag{28}$$

Thus, the lifetime of the quasibound state with wave number $k$ is given by the imaginary part of Eq. (27).

### C. Quantum supercavity

In Fig. 5, we show the numerically obtained spatial distribution of the photon wave function along the CRW for a given $k$ in Eq. (27). In Fig. 6, we also give the corresponding schematic explanation for the establishment of the supercavity of Fig. 5. In Fig. 6, the eigenenergy $\omega$ of the cavity at the site $j=\pm d$ is shown by green dashed lines, and the atomic transition energy $\Omega$ is shown by the red dashed lines. The eigenvalues of two dressed states are denoted by the symbols $\varepsilon_{\pm}$. The blue solid lines present the energy band formed by other resonators. From Fig. 5, it can be found that a well-localized state appears in the sandwiched segment as long as the coupling strength $J$ is much larger than the hopping energy $\xi$ and the detuning $\delta=\omega-\Omega$, as shown in Fig. 5(a). In this situation, the coupling strength $J$ plays a dominant role, and thus the coupling $J$ shifts the energies at $j=\pm d$ to

$$\varepsilon_{\pm} = \tfrac{1}{2}[\omega + \Omega \pm \sqrt{(\omega-\Omega)^2 + 4J^2}]. \tag{29}$$

When $\omega=\Omega$, the two strong $J$ couplings split the original degenerate energies of the cavity and the single atomic-excited state into two new dressed states at the point $j=\pm d$. These two dressed states are outside the energy band of the incident photon, as shown in Fig. 6(a). Therefore, the photons will have a very low probability of going through the atoms, since the resonance condition is not satisfied in Fig. 6(a). Thus, if a photon is initially located between the two atoms, it will remain there, bouncing back and forth from the atoms. The wave functions shown in Figs. 5(b) and 5(c) also indicate that a supercavity can be formed, but the leakage of this quantum supercavity is larger than in Fig. 5(a). The reason for this large leakage in Fig. 5(c) and especially in Fig. 5(b) lies in the energy diagram of Fig. 6. Although the coupling strength is much larger than the hopping constant $\xi$ in Figs. 5(b) and 5(c), the original eigenfrequencies, described by $\omega$ and $\Omega$ in Fig. 6(b), are shifted in opposite directions to $\varepsilon_{\pm}$, but this shift amount $(\varepsilon_+-\omega)$ is still inside the band, therefore the tunneling process may appear with larger probability than the case in Fig. 6(a). Comparing Fig. 5(b) with Fig. 5(c), it shows that the probability for a single photon in the outside region in Fig. 5(b) is larger than that in Fig. 5(c). Figures 5(b) and 5(c) further show the relation between the magnitude $J^2/\delta$ and the half-width $2\xi$. When $\delta \gg J$ and $J>\xi$, the dominant photon-atom couplings approximately shifts the energy of the cavity to

$$\varepsilon_+ \approx \omega + \frac{J^2}{2\delta}. \tag{30}$$

Indeed, Figs. 5(b) and 5(c) show the change of the resonant states when $J^2/\delta$ approaches $2\xi$, e.g., the relation between the dressed state $\varepsilon_+$ and the upper edge of the band. Obviously, the dressed energy level $\varepsilon_+$ is closer to the edge of the band in Fig. 5(c) than the one in Fig. 5(b), therefore, the probability is much smaller in Fig. 5(c) for a photon to be outside the sandwiched segment. Therefore, each atom plays the role of a partially reflecting mirror. Here, we present a way to tune the leakage of the quantum supercavity.

### D. Quantum supercavity with $\Omega$ inside the band

The supercavity was studied above for large coupling strength $J$. As long as $J$ is nonzero, *a perfect reflection appears when the energy of the incident photon matches the transition energy of the atom* [17]. Therefore, a perfect supercavity exists regardless of the magnitude of $J$. Of course, a perfect supercavity $(r=1)$ is an ideal limiting case. In reality, decoherence and losses will make the reflection coefficient $r<1$.

The photon trapping energy can be found analytically, since Eq. (24) holds exactly when the transition frequency $\Omega$ satisfies the condition

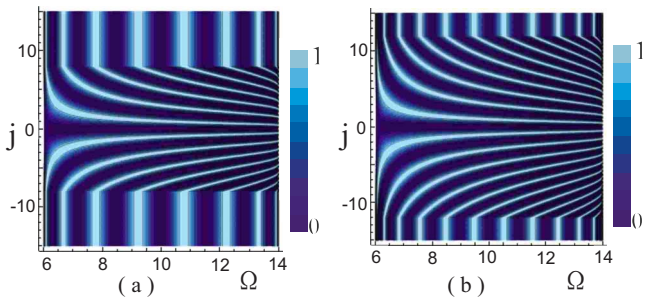


FIG. 7. (Color online) Contour plots of the norm square of the wave function $u_k(j)$ with odd parity versus the position along the CRW and the atomic transition energies $\Omega$, where $\Omega$ is assumed to be inside the band. Here, $\xi=2$, $\omega=10$, $d=8$ for (a) and $d=12$ for (b).

$$\Omega = \omega - 2\xi \cos(q_n/2) \tag{31}$$

and the corresponding resonant state has wave numbers $k=q_n/2$. Thus, in this case, the two atoms form two mirrors with perfect reflection, which leads to a perfect supercavity.

Figure 7 shows the contour plots of the probability for a single photon as a function of the coordinate $j$ along the CRW and for the transition energy $\Omega$. Here, the atomic transition energy $\Omega$ is assumed to be inside the energy band of the CRW. Also only the wave function $u_k(j)$ with odd parity is depicted in Fig. 7, which is the reason why the probability $|u_k(j)|^2$ is zero at $j=0$. If one regards the segment between the two atoms as a finite chain with $N=2d$ sites, the wave number in this segment takes $N$ discrete values, which give rise to the discrete energy levels. Figure 7 shows that when the transition energy $\Omega$ *matches* one of the discrete energy levels in the segment sandwiched by the two atoms, *bound states* appear and a *quantum supercavity* is formed. These bound states are independent of the coupling strength $J$; however, a nonzero $J$ is necessary.

### E. Quantum supercavity made of superconducting qubits

Using superconducting charge qubits (one kind of "artificial atom") as an example, we now focus on the question on trapping and reemitting photons in this unusual type of atomic resonator. It is well known that the transition frequency $\Omega$ of superconducting charge qubits can be controlled by both the voltage applied to the gate and the external flux through the SQUID loop [32–34]. Let us assume that a photon with energy

$$E_k = E_n = \omega - 2\xi \cos q_n \tag{32}$$

is initially in the $(-d)$th cavity. First, we tune the transition frequency $\Omega$ outside the energy band and consider a large detuning $(\Omega - E_n)$. When the photon meets the first qubit, it passes the first qubit and moves freely beyond the first qubit due to the large detuning. After the photon is inside the spatial range $[-d,d]$ between the two qubits, the transition frequencies $\Omega_1=\Omega_2=\Omega$ are adjusted inside the energy band, and satisfy Eq. (31). Therefore the photon would be totally trapped inside the supercavity. We note that a tunable supercavity could also be obtained by doping two $\Lambda$-type atoms inside the coupled-cavity array [35].

Based on the previous discussion in this paper, we can conclude the following: (1) The single-photon can be trapped in the region $[-d,d]$ with a finite lifetime; (2) the single-photon can get out of the atomic resonator when the transition frequencies $\Omega$ of these two atoms are not equal to the incident energy of the single photon. In the appendix we will show that the existence of the photon bound states between the two atomic mirrors is independent of the magnitude of the transition energy $\Omega$. We also conclude that a new cavity is formed by the two atoms separately embedded in the two cavities of the coupled-cavity array. Therefore, in analogy with superlattices in solid state, we call this cavity a *supercavity* and the atoms act as *atomic mirrors*.

## V. LONG-WAVELENGTH EFFECTIVE THEORY

In this section, we show that the real part of the momenta of the quasibound levels in the low-energy region can be obtained by expanding the sine and cosine functions in Eq. (26) as $\sin q_n \approx q_n$ and $\cos q_n \approx 1-q_n^2/2$. Low-energy photons propagating along the resonator waveguide have long wavelengths. Under the long-wavelength approximation, a quadratic spectrum

$$E_k^L = \omega_\xi + \xi k^2 \tag{33}$$

is found by expanding the cosine function around zero in Eq. (7), where the superscript $L$ in $E_k^L$ refers to the long-wavelength or lower-energy regime and $\omega_\xi=\omega-2\xi$. By introducing the field operator

$$\varphi(x) \equiv \int_{-\infty}^{\infty} dk \exp(ikx) a_k \tag{34}$$

with the commutation relation

$$[\varphi(x), \varphi^\dagger(x')] = \delta(x-x'), \tag{35}$$

the Hamiltonian of the system in real space becomes

$$H = \int_{-\infty}^{\infty} dx \varphi^\dagger(\omega_\xi - \xi\partial_x^2)\varphi + \sum_l \left( \Omega |e\rangle_l\langle e| + J\int_{-\infty}^{\infty} dx \delta[x+(-1)^l d](\varphi^\dagger S_l^- + \text{H.c.}) \right), \tag{36}$$

where $S_l^- = |g\rangle_l\langle e|$ is the spin lowering operator of the $l$th atom. Since the total number of excitations is conserved, we consider the storage of a single photon in the region separated a distance $2d$ by two $\delta$ potentials. In the coordinate representation, the stationary state of the system

$$|E_k^L\rangle = \int_{-\infty}^{\infty} dx u_k(x)\varphi^\dagger(x)|0gg\rangle + u_{k1e}^{\text{long}}|0eg\rangle + u_{k2e}^{\text{long}}|0ge\rangle \tag{37}$$

is the superposition of a single photon (first term) and the single-excited states of the two atoms (second and third terms). The effective equation for the photon

$$JG_k[\delta(x-d)u_k(d)+\delta(x+d)u_k(-d)]=(\xi\partial_x^2+E_k^L-\omega_\xi)u_k(x) \tag{38}$$

is achieved from the eigenvalue equation $H|E_k^L\rangle=E_k^L|E_k^L\rangle$. Two $\delta$ potentials appear in Eq. (38) along the direction of the photon propagation, one is located at $x=-d$ and the other is located at $x=d$. The height of the potential is dependent on the energy carried by a single photon. These two atoms divide the region of photon propagation into three zones: (I) $x<-d$; (II) $-d<x<d$; (III) $x>d$. The effective Hamiltonian

$$H_{\text{eff}}=\omega_\xi-\xi\partial_x^2, \tag{39}$$

is valid in all three zones, and corresponds to free-particle Schrödinger equations, except for the replacement of $E_k^L$ by $(E_k^L-\omega_\xi)$ in $H|E_k^L\rangle=E_k^L|E_k^L\rangle$.

We now concentrate on the case $E_k^L>\omega_\xi$. From the standard boundary conditions that a wave function is always continuous and its derivative is continuous except at points where the potential is infinite, we can derive the continuity equations for wave function $u_k(x)$ in different zones, and the discontinuity of its derivatives (slopes) at the points $x=\pm d$. According to the symmetry of the system, we assume that Eq. (38) has the following solution:

$$u_k(x)=\begin{cases} S_1e^{-ikx}, & x<-d, \\ e^{ikx}+B_Le^{-ikx}, & -d<x<d, \\ S_2e^{ikx}, & x>d. \end{cases} \tag{40}$$

Using the same approach described in Sec. IV, we obtain the coefficients

$$S_1=\frac{k\xi e^{-i2kd}+JG_k^L\sin(2kd)}{2k\xi+iJG_k^L}, \tag{41a}$$

$$S_2=\frac{k\xi}{2k\xi+iJG_k^L}, \tag{41b}$$

$$B_L=\frac{JG_k^Le^{i2kd}}{2ik\xi-JG_k^L}, \tag{41c}$$

with $G_k^L=J/(E_k^L-\Omega)$ and the condition for the existence of the resonant states

$$e^{i2kd}=\pm\frac{2i\xi}{J^2}k(E_k^L-\Omega)\mp 1. \tag{42}$$

Here the wave number $k$ is complex. Under the condition $Q=2\xi^2/(J^2d^3)\ll 1$, the wave number

$$k=q_n-\frac{1}{2}Q_n^L+d(Q_n^L)^2+i\frac{\lambda}{2d}Q_n^L(\delta_\xi+3\xi q_n^2)+O(Q^3) \tag{43}$$

is approximately obtained, up to second order in the parameter $Q$, for those states with odd parity, and

$$Q_n^L=\frac{\lambda q_n}{d}(\omega-2\xi-\Omega+\xi q_n^2). \tag{44}$$

The superindex $L$ in Eqs. (43) and (44) refers to the low-energy regime (long-wavelength approximation) studied in this section. The real part, $\text{Re}(k)$, and the imaginary part, $\text{Im}(k)$ in Eq. (43) of a quasibound state provide the energy and the lifetime of this state via the dispersion relation in Eq. (33). It is clear that the $\text{Re}(k)$ can be obtained by expanding the sine and cosine functions around zero. Obviously, when $k=q_n$ and $\Omega=\omega_\xi+\xi k^2$, a perfect cavity is formed. In this case, the coefficients $S_1$ and $S_2$ are zero. In Fig. 8, the probability for finding a photon in space is shown. As the transition energy $\Omega$ varies, the effective potential induced by the two qubits changes from barriers to wells. It can be found that, as the depth or height of the $\delta$ potential becomes larger, the leakage of the supercavity becomes smaller, which offers a way to control the leakage of the supercavity by adjusting the energy level spacing of the two qubits. Therefore, single photons can be trapped.

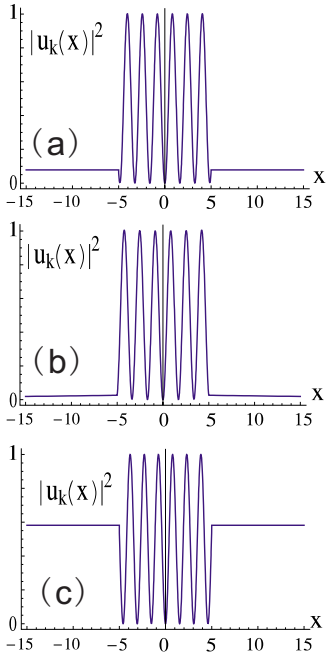


FIG. 8. (Color online) The probability $|u_k(x)|$ for finding the photon in space using the long-wavelength effective theory. The distance between qubits is $2d=10$. Other parameters are in units of $J$. $\xi=0.1$, $n=3$, $\omega=5$ (a) $\Omega=3$, (b) $\Omega=4$, (c) $\Omega=7$. For a given $n$, $q_n=\frac{n\pi}{d}$. These were the inputs to Eqs. (43) and (44), which provide $Q_n^L$ and $k$. With this $k$, Eqs. (40)–(42) are used to obtain the $u_k(x)$'s shown in the figures.

## VI. SHORT-WAVELENGTH EFFECTIVE THEORY

In the higher-energy regime, the short-wavelength approximation leads to a linear spectrum $E_k=\omega_\pi+2\xi|k|$, with $\omega_\pi=\omega-\pi\xi$. Introducing the left [right] bosonic field operator $\varphi_L^\dagger(x)$ $[\varphi_R^\dagger(x)]$, which creates a left-moving [right-moving] particle at $x$, the tight-binding Hamiltonian now becomes

$$H_c=\omega_\pi\sum_{\alpha=R,L}\int_{-\infty}^{\infty}dx\varphi_\alpha^\dagger(x)\varphi_\alpha(x)+2i\xi\int_{-\infty}^{\infty}dx[\varphi_R^\dagger(x)\partial_x\varphi_R(x) - \varphi_L^\dagger(x)\partial_x\varphi_L(x)]. \tag{45}$$

The left-moving and right-moving fields interact with these

atoms, respectively, therefore the interaction Hamiltonian becomes

$$H_I = J\sum_{\alpha l}\int_{-\infty}^{\infty} dx\,\delta[x+(-)^l d][\varphi_\alpha^\dagger(x)S_l^- + \text{H.c.}] + \Omega\sum_l |e\rangle_l\langle e|. \tag{46}$$

Although the Hamiltonian in the short-wavelength regime (linear dispersion regime) is significantly different from previous ones, the number of total excitations is still a conserved quantity. The stationary state for $H=H_c+H_I$ with one particle excitation takes the form

$$|E_k^S\rangle = \sum_\alpha \int dx u_{k\alpha}(x)\varphi_\alpha^\dagger(x)|0gg\rangle + u_{1e}|0eg\rangle + u_{2e}|0ge\rangle, \tag{47}$$

where the first number 0 in the Dirac bracket represents the vacuum state of the cavity fields. Hereafter, the superindex "$S$" will refer to the short-wavelength approximation regime. $u_{kR}(x)$ and $u_{kL}(x)$ represent the probability amplitudes for finding the photon along the right-moving and left-moving direction at position $x$. Moreover, $u_{je}$ (with $j=1,2$) are the probability amplitudes for one qubit in the excited state and the other one in the ground state. From the Schrödinger equation, we obtain the relation between the left-moving amplitude and the atomic amplitude in the excited state

$$(E_k^S - \omega_\pi - 2i\xi\partial_x)u_{kL} = J\sum_j \delta[x+(-)^j d]u_{je}. \tag{48}$$

The relation between the right-moving amplitude and the atomic amplitude is

$$(E_k^S - \omega_\pi + 2i\xi\partial_x)u_{kR} = J\sum_j \delta[x+(-)^j d]u_{je}. \tag{49}$$

We can also find that the atomic amplitude $u_{je}$, the right-going amplitude $u_{kR}$, and left-moving amplitudes $u_{kL}$ satisfy the relation

$$u_{je} = G_k^S\int_{-\infty}^{\infty} dx\,\delta[x+(-)^j d](u_{kR}+u_{kL}), \tag{50}$$

with the Green function $G_k^S=J/(E_k^S-\Omega)$. After eliminating the variables $u_{1e}$ and $u_{2e}$, both the left-moving eigenfunction

$$\begin{aligned}(E_k^S - \omega_\pi - i2\xi\partial_x)u_{kL}(x) = {} & JG_k^S\delta(x-d)\int_{-\infty}^{\infty} dx'\,\delta(x'-d)\\ & \times[u_{kR}(x')+u_{kL}(x')] + JG_k^S\delta(x\\ & + d)\int_{-\infty}^{\infty} dx'\,\delta(x'+d)[u_{kR}(x')\\ & + u_{kL}(x')]\end{aligned} \tag{51}$$

and right-moving eigenfunction

$$\begin{aligned}(E_k^S - \omega_\pi + i2\xi\partial_x)u_{kR}(x) = {} & JG_k^S\delta(x-d)\int_{-\infty}^{\infty} dx'\,\delta(x'-d)\\ & \times[u_{kR}(x')+u_{kL}(x')] + JG_k^S\delta(x\\ & + d)\int_{-\infty}^{\infty} dx'\,\delta(x'+d)[u_{kR}(x')\\ & + u_{kL}(x')]\end{aligned} \tag{52}$$

are subjected to a $\delta$ potential with singularities at $x=\pm d$.

In the region $x\neq\pm d$, the potential is zero, and the solutions of Eqs. (52) and (53) are plane waves with left-moving and right-moving wave-vector number $k=E_k^S/v_g$. Therefore, we can assume the right-moving

$$u_{kR}(x) = \begin{cases} 0, & x<-d,\\ e^{ikx}, & -d<x<d,\\ t_R e^{ikx}, & x>d,\end{cases} \tag{53}$$

and the left-moving wave function

$$u_{kL}(x) = \begin{cases} t_L e^{-ikx}, & x<-d,\\ r_L e^{-ikx}, & -d<x<d,\\ 0, & x>d,\end{cases} \tag{54}$$

which allow the existence of quasibound states in this system. The magnitude of $r_L$

$$r_L = \frac{JG_k^S}{i2\xi - JG_k^S}e^{i2kd} = \frac{i2\xi - JG_k^S}{JG_k^S}e^{-i2kd} \tag{55}$$

and the relations

$$t_R = r_L e^{-i2kd} + 1, \tag{56a}$$

$$t_L = r_L + e^{-i2kd} \tag{56b}$$

of the amplitudes $t_R$, $t_L$, and $r_L$ can be obtained by integrating Eqs. (51) and (52) in the neighborhood of $x=\pm d$. For the appearance of quasibound states in the spatial range sandwiched by two atoms, Eq. (55) leads to the condition

$$e^{2ikd} = \pm\frac{2i\xi}{JG_k^S} \mp 1 \tag{57}$$

with the complex wave number $k$. Here, the lower sign corresponds to the odd parity, and the upper sign corresponds to the even parity. Obviously, when the transition energies $\Omega$ of the two atoms are

$$\Omega = \omega_\pi + 2\xi\left|\frac{n\pi}{d}\right|, \tag{58}$$

the bound states have odd parity. However the even parity corresponds to the transition energy

$$\Omega = \omega_\pi + 2\xi\left|\frac{\pi}{d}\left(n+\frac{1}{2}\right)\right|. \tag{59}$$

Except for the situation discussed above, Eq. (57) does not have an exact solution. We now seek the values of $k$ for which Eq. (57) can be approximately solved. Here we only

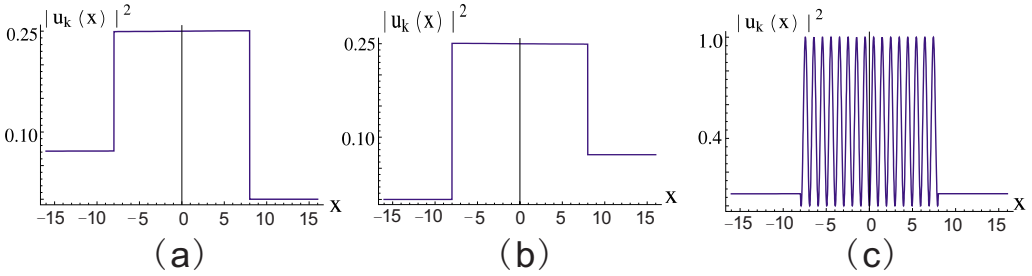


FIG. 9. (Color online) The norm square of the left-moving wave function $|u_{kL}(j)|^2$ (a), the right-moving wave function $|u_{kR}(j)|^2$ (b), and probability $|u_k(j)|^2 \equiv |u_{kL}(j)+u_{kR}(j)|^2$ (c) for finding the photon in space. The parameters are set as follows: $d=8$, $\xi=0.1$, $n=1$, $\omega=5$, $\Omega=2$. Parameters are in units of $J$. For a given $n$, $q_n=\frac{n\pi}{d}$. These were the inputs to Eqs. (60) and (61), which provide $Q_n^H$ and $k$. With this $k$, Eqs. (53)–(57) are used to obtain the $u_k(x)$'s shown in (a)–(c).

consider the energy levels with odd parity. A similar calculation provides results for even parity. Using the approach described above with the parameter $P=4\xi^2/(dJ^2)$ and $\lambda=2\xi/J^2$, Eq. (57) with the lower sign, yields the wave number

$$k \approx q_n - \frac{J}{2d}Q_n^S + d(Q_n^S)^2 + i\xi\frac{\lambda}{d}Q_n^S + O(P^3) \tag{60}$$

whose real part can be obtained from Eq. (29) by expanding the sine and cosine functions as $\sin q_n \approx 1$ and $\cos q_n$ around $\pi/2$. Here,

$$Q_n^S = \frac{\lambda}{d}(\delta_\pi + 2\xi q_n) \tag{61}$$

and

$$\delta_\pi = \omega - \pi\xi - \Omega. \tag{62}$$

We plot the norm square of the left-going wave function in Fig. 9(a), the right-going wave function in Fig. 9(b), and the total wave function $u_k(j)$ in Fig. 9(c), where $u_k(j) \equiv u_{kL}(j) + u_{kR}(j)$.

## VII. CONCLUSIONS

We have studied the coherent control of single photon transfer in a coupled resonator waveguide with two atoms. The coherent control can be realized by adjusting the detuning between the single photon frequency and the energy-level-spacings of the atoms. We have shown that a supercavity is formed in the coupled-cavity array due to the strong coupling between the atoms and the corresponding cavities, and the discrete values of the photon momenta are analytically derived. Moreover, a perfect supercavity appears when the transition energies of the two atoms are equal to the energy of an incident photon. We also find that besides the bound states formed by two perfect atomic mirrors, there always exist other bound states at the edge of the band. The real parts of the discrete momenta obtained by the discrete approach unify those obtained by the effective continuum theory in both the long-wavelength and short-wavelength regions.

## ACKNOWLEDGMENTS

This work is supported in part by NSFC Grants No. 90203018, No. 10474104, No. 60433050, No. 10775048 and No. 10704023, NFRPC Grant No. 2006CB921205, No. 2007CB925204, and No. 2005CB724508. F.N. acknowledges partial support from the National Security Agency, Laboratory Physical Science, Army Research Office, National Science Foundation Grant No. EIA-0130383, JSPS-RFBR Contract No. 06-02-91200, and Core-to-Core program supported by the Japan Society for Promotion of Science (JSPS). One of the authors (L.Z.) acknowledges useful discussions with S. Ashhab.

## APPENDIX: PHOTON BOUND STATES BETWEEN TWO ATOMIC MIRRORS

To find the wave functions for the eigenvalue equation (18), one needs to write the wave functions in different regions. Since exchanging of the two atoms does not change the equations for the wave functions of the photon propagating along the CRW, here we only deal with odd-parity wave functions, which have the sinh function in the center region and exponential decay in the edge regions

$$\Psi_-(x) = \begin{cases} -A\exp[(in\pi+\kappa)j], & x<-d, \\ B\exp(in\pi j)\sinh(\kappa j), & -d<x<d, \\ A\exp[(in\pi-\kappa)j], & x>d. \end{cases} \tag{A1}$$

From the continuity and discontinuity conditions at $x=d$,

$$u(d^+) = u(d^-),$$

$$(\omega + JG_\kappa - E)u(d) = \xi[u(d+1)+u(d-1)],$$

we can easily obtain

$$\tanh(\kappa d) = \frac{\xi\exp(-in\pi)\sinh\kappa}{E-\omega-JG+\xi(e^{in\pi-\kappa}+e^{-in\pi}\cosh\kappa)} \tag{A2}$$

with

$$E_\kappa = \omega - \xi(e^{in\pi-\kappa} + e^{-in\pi+\kappa})$$

and

$$G_\kappa = \frac{J}{E_\kappa - \Omega}.$$

In principle, $\kappa$ can be obtained by solving the implicit transcendental equation (A2). It is obvious that $\kappa=0$ is one of the solutions of Eq. (A2). This $\kappa=0$ solution makes sure that the odd-parity wave functions exist and two bound states appear at the edges.


[1] S. E. Harris, Phys. Today **50**(7), 36 (1997).
[2] M. Fleischhauer and M. D. Lukin, Phys. Rev. Lett. **84**, 5094 (2000); Phys. Rev. A **65**, 022314 (2002).
[3] C. P. Sun, Y. Li, and X. F. Liu, Phys. Rev. Lett. **91**, 147903 (2003).
[4] T. W. Mossberg, Opt. Lett. **7**, 77 (1982).
[5] H. Lin, T. Wang, and T. W. Mossberg, Opt. Lett. **20**, 1658 (1995).
[6] B. Kraus, W. Tittel, N. Gisin, M. Nilsson, S. Kröll, and J. I. Cirac, Phys. Rev. A **73**, 020302(R) (2006).
[7] K. J. Vahala, Nature (London) **424**, 839 (2003).
[8] J. Bravo-Abad and M. Soljačić, Nature Mater. **6**, 799 (2007).
[9] Y. Tanaka, J. Upham, T. Nagashima, T. Sugiya, T. Asano, and S. Noda, Nature Mater. **6**, 862 (2007).
[10] M. Sandberg, C. M. Wilson, F. Persson, T. Bauch, G. Johansson, V. Shumeiko, T. Duty, and P. Delsing, Appl. Phys. Lett. **92**, 203501 (2008).
[11] M. A. Castellanos-Beltran and K. W. Lehnert, Appl. Phys. Lett. **91**, 083509 (2007).
[12] J. Kim, O. Benson, H. Kan, and Y. Yamamoto, Nature (London) **397**, 500 (1998).
[13] B. Dayan, A. S. Parkins, T. Aoki, E. P. Ostby, K. J. Vahala, and H. J. Kimble, Science **319**, 1062 (2008).
[14] F. Y. Hong and S. J. Xiong, Phys. Rev. A **78**, 013812 (2008).
[15] D. E. Chang, A. S. Sørensen, E. A. Demler, and M. D. Lukin, Nat. Phys. **3**, 807 (2007).
[16] J. T. Shen and S. Fan, Phys. Rev. Lett. **95**, 213001 (2005); **98**, 153003 (2007); Opt. Lett. **30**, 2001 (2005).
[17] L. Zhou, Z. R. Gong, Y. X. Liu, C. P. Sun, and F. Nori, Phys. Rev. Lett. **101**, 100501 (2008).
[18] H. Dong, Z. R. Gong, H. Ian, L. Zhou, and C. P. Sun, e-print arXiv:0805.3085.
[19] C. P. Sun, L. F. Wei, Y. X. Liu, and F. Nori, Phys. Rev. A **73**, 022318 (2006).
[20] M. Mariantoni, F. Deppe, A. Marx, R. Gross, F. K. Wilhelm, and E. Solano, Phys. Rev. B **78**, 104508 (2008).
[21] A. Greentree, C. Tahan, J. H. Cole, and L. C. L. Hollenberg, Nat. Phys. **2**, 856 (2006).
[22] D. G. Angelakis, M. F. Santos, and S. Bose, Phys. Rev. A **76**, 031805(R) (2007).
[23] L. Zhou, J. Lu, and C. P. Sun, Phys. Rev. A **76**, 012313 (2007).
[24] F. M. Hu, L. Zhou, T. Shi, and C. P. Sun, Phys. Rev. A **76**, 013819 (2007).
[25] M. J. Hartmann, F. G. S. L. Brandão, and M. B. Plenio, Nat. Phys. **2**, 849 (2006).
[26] A. L. Rakhmanov, A. M. Zagoskin, S. Savel'ev, and F. Nori, Phys. Rev. B **77**, 144507 (2008).
[27] K. Yu. Bliokh, Yu. P. Bliokh, V. Freilikher, S. Savel'ev, and F. Nori, Rev. Mod. Phys. **80**, 1201 (2008).
[28] F. Ciccarello, G. M. Palma, M. Zarcone, Y. Omar, and V. R. Vieira, J. Phys. A **40**, 7993 (2007); Laser Phys. **17**, 889 (2007); New J. Phys. **8**, 214 (2006).
[29] F. M. Dittes, Phys. Rep. **339**, 215 (2000).
[30] Y. S. Joe, A. M. Satanin, and G. Klimeck, Phys. Rev. B **72**, 115310 (2005).
[31] N. Hatano, K. Sasada, H. Nakamura, and T. Petrosky, Prog. Theor. Phys. **119**, 187 (2008); e-print arXiv:0705.1388.
[32] J. Q. You and F. Nori, Phys. Today **58**(11), 42 (2005).
[33] J. Q. You and F. Nori, Phys. Rev. B **68**, 064509 (2003).
[34] Y. X. Liu, L. F. Wei, and F. Nori, Phys. Rev. A **71**, 063820 (2005).
[35] Z. R. Gong, H. Ian, Lan Zhou, and C. P. Sun, Phys. Rev. A **78**, 053806 (2008).